FEBS 30143 FEBS Letters 579 (2005) 6575–6580

FM1–43 measurements of local exocytotic events in rat melanotrophs

S.K. Sikdar[a,c,1], M. Kreft[a,b,1], T. Pangrsic[a], S. Grilc[a], R. Zorec[a,b,*]

[a] *Laboratory of Neuroendocrinology-Molecular Cell Physiology, Institute of Pathophysiology, Medical Faculty, University of Ljubljana Medical School, Zaloska 4, SI-1000 Ljubljana, Slovenia*
[b] *Celica Biomedical Sciences Center, Stegne 21, Ljubljana, Slovenia*
[c] *Molecular Biophysics Unit, Indian Institute of Science, Bangalore 560 012, India*

Received 23 August 2005; revised 11 October 2005; accepted 25 October 2005

Available online 9 November 2005

Edited by Felix Wieland

Abstract **We have explored the existence of fusion- and secretion-competent sites on the plasma membrane of peptide secreting rat pituitary melanotrophs at rest, and following stimulation with glutamate. We monitored changes in fluorescence of FM1–43, a styryl dye which labels plasma membrane. The results show spontaneous local increases in FM1–43 reporting changes in membrane surface area due to cumulative exocytosis. Addition of glutamate, further increased the occurrence of these events. Statistical analysis of local FM1–43 fluorescence changes suggests that this is due to the recruitment of inactive exocytotic domains and due to the stimulation of already active exocytotic domains.**

Keywords: Neuroendocrine cell; Exocytosis; FM1–43; Hormone secretion; Exocytotic domain

1. Introduction

The melanotrophs, neuroendocrine cells from the pituitary *pars intermedia* exhibit substantial spontaneous secretion in cell culture [1]. The spontaneous secretion is reduced by the neurotransmitters dopamine and γ-aminobutyric acid, present in the hypothalamic neurons innervating the intermediate lobe [2]. In addition, an excitatory glutamatergic innervation has been suggested to affect the secretion of peptide hormones from these cells. Glutamate and glutamate specific receptor agonists have been shown to cause a rise in intracellular $[Ca^{2+}]$ in the rat melanotrophs suggesting the presence of ionotropic NMDA and non-NMDA AMPA/K receptors, but not the metabotropic glutamate receptors [3]. The final stage of secretion in these cells is mediated by fusion of the secretory vesicle with the plasma membrane. This has been examined earlier by monitoring rapid changes in membrane surface area as jumps in membrane capacitance [4,5], and by amperometry [6,7].

The number of secretory vesicles in a single neuroendocrine cell is about 40–80 000. However, only ~1% of them, representing a ready releasable pool, can be exocytosed upon stimulation [4,8–10]. Electron microscopy examinations [10,11] provided conflicting evidence of specialized accumulations of apparently docked vesicles on the plasma membrane in endocrine cells.

It is possible that the number of vesicles that actually fuse with the plasma membrane is tightly regulated by the number of sites on the plasma membrane where fusion of vesicles can occur at any given moment in time. Such special structures have been identified for exocytotic fusion of single synaptic vesicles in the presynaptic nerve terminal of retinal bipolar neurons by total internal reflection fluorescence microscopy [12]. However, other experimental evidence obtained on chromaffin neuroendocrine cells is somehow controversial. On one hand there are results that are not in favour of specialized release sites. Cuchillo-Ibanez et al. [13] showed that isolated chromaffin cells only exhibit a polarised catecholamine release, occurring in the bottom of the cells, compared to equatorial or apex planes. Each individual granule associates with its own random release site [14] or secretion is preferential in the terminals of neurite-emitting chromaffin cells [15]. On the other hand, some studies point to the existence of specialized release sites in neuroendocrine cells. Amperometrical spatial mapping of the catecholamine release [16] in conjunction with Ca^{2+} imaging showed colocalization in distinct release sites of chromaffin cells [17,18]. These studies employed an indirect mapping of release at a fair distance from the plasma membrane and it would have been ideal if one was able to monitor exocytosis at locales where release of substances was occurring directly. An ideal strategy is to use FM1–43, a vital membrane styryl dye which reports cumulative exocytosis [19,20]. Styryl dyes are amphiphilic and fluoresce when inserted into hydrophobic environment, such as the plasma membrane, but can not cross the membrane bilayer. Therefore, an increase in the cell membrane area can readily be reported by these dyes.

In the present work, we studied the existence of specific fusion- and secretion-competent sites in the plasma membrane of peptide secreting neuroendocrine cells. We asked whether cell stimulation results in enhanced fusion of vesicles at specialized membrane locales termed exocytotic domains, as observed in nerve terminals [12], or does the release phenomenon become more diffuse where the cell uses the plasma membrane for exocytosis unspecifically.

Neuroendocrine melanotrophs from the intermediate lobe of the rat pituitary gland secrete the peptide hormones α-melanocyte stimulating hormone (α-MSH) and β-endorphin [21]. The number of secretory vesicles in a single melanotroph is about 60 000, and only a few thousand of them

*Corresponding author. Fax: +386 1 543 7036.
E-mail address: robert.zorec@mf.uni-lj.si (R. Zorec).

[1] These authors contributed equally to this work.

0014-5793/$30.00
doi:10.1016/j.febslet.2005.10.049

are close to the plasma membrane [9]. The expected frequency of exocytotic events was estimated to be about 4000 per second [4], meaning thereby that only a fraction of the secretory vesicles actually undergo fusion at any given time.

The results of the present study show that the plasma membrane, stained by FM1–43, exhibits spontaneous and glutamate-stimulated increases in fluorescent intensity, which is localized to distinct membrane areas. The experimental evidence is consistent with the view that the peptide secretory activity in rat melanotrophs is mediated via specific exocytotic domains, specialized fusion- and secretion-competent sites in the plasma membrane.

2. Materials and methods

2.1. Cell culture, immunofluorescence and FM1–43 imaging

Rat pituitary melanotrophs were prepared as described previously [22]. The external bath solution contained (in mM): NaCl 131.8, $CaCl_2 \cdot 2H_2O$ 5, KCl 5, $MgCl_2 \cdot 6H_2O$ 2, HEPES/NaOH 10, D-glucose 10, $NaH_2PO_4 \cdot 2H_2O$ 0.5, $NaHCO_3$ 5; pH 7.2. For dynamic fluorescence imaging, melanotrophs plated onto glass coverslips were washed in external solution, mounted onto the recording chamber, and transferred onto the stage of the confocal microscope, and a DIC image of the cells to be scanned for FM1–43 fluorescence was acquired. The external solution was exchanged for an equal volume of 5 μM FM1–43 containing external solution. The time between the exchange of external solution with FM1–43 and the commencement of scanning was kept the same in all the experiments. Further, in all the experiments FM1–43 was left present in the bath. Dopamine at 200 nM concentration was included in the recording solutions to increase the percentage of cells that respond to glutamate [3] and to reduce basal secretion [2]. Optical sections were taken approximately closer to the equatorial region of the cell.

2.2. Confocal imaging

The cells were imaged on an inverted microscope (Zeiss 510 with ×63, 1.4 NA oil objective) coupled to a Zeiss 510 laser scanning confocal system (excitation, 488 nm), emission (505 nm and above). The confocal system was used in the *xy* scan mode (512 pixels in *x* and *y*, pixel resolution, 0.07 μm; acquisition time, 1.5 s, continuous). The confocal aperture was set to 2 times the airy disc, which corresponded to 25% of maximal opening. The resolution was estimated to be 2 μm in the *z* dimension, and about 440 nm in the *x* and *y* dimensions. Melanotrophs were randomly selected and 2–3 cells were positioned in the field. Glutamate was prepared in the external bath solution and added as a concentrated bolus to achieve a bath concentration of 400 μM. Control experiments consisted of similar applications of bath solution. All distributions resulting from experimental manipulations are compared to a baseline distribution.

Circular patches of cell surface membrane of 2 μm diameter (30 pixels in diameter, pixel resolution 0.07 μm) were analyzed for fluorescence excluding bright spots on the membrane surface (Figs. 1A, 2A, arrowheads) due to debris or deposited secretory granule content [20]. Regions of cell surface membranes, which showed any movements of the focal plane, were discarded from analysis. The scanning duration in an experimental run lasted for not more than 3 min. In all the analysis reported in Fig. 3, spots that showed continued exponential decrease beyond 40 s were excluded from analysis, since these represented events related to photobleaching of primed endocytosed vesicles or incomplete equilibration of the cell membrane with FM1–43 [20].

2.3. Experimental animals

Adult wistar rats were used for the study, and were euthanized with carbon-di-oxide. The authors' institutional committee on animal care approved the studies.

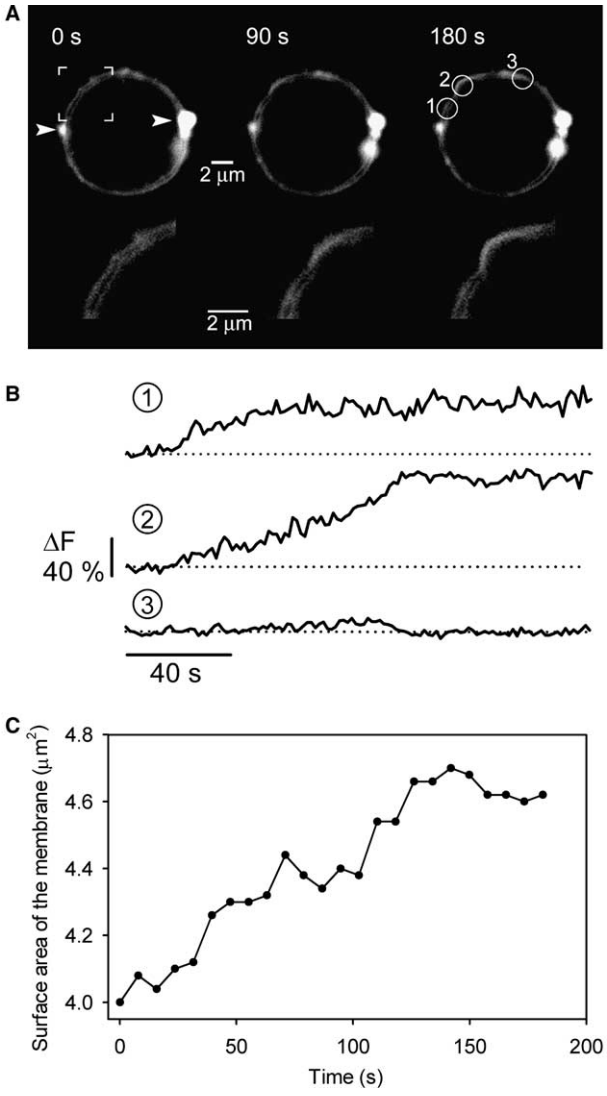

Fig. 1. Localized increase in FM1–43 fluorescence intensity is accompanied by an increase in membrane area. (A) Confocal *xy* fluorescence image of a single melanotroph stained by FM1–43 (5 μM), at three different time periods (indicated on upper set of panels). The frame indicates the magnified region of the cell membrane (insets below) to highlight the local increase in fluorescence intensity and the accompanying increase in membrane surface area. Arrowheads mark the bright spots on the membrane surface, representing hormone deposition on the cell surface, which were discarded from the analysis. (B) Time-dependent changes in the plasma membrane fluorescence intensity. The plots are from the regions marked by the circles on the membrane of the cell (panel A). The horizontal scale bar represents time of 40 s and the vertical scale bar represents the 40% change of fluorescence relative to the basal fluorescence of the region of interest. (C) The change in membrane surface area is plotted against time, at the membrane region (frame in panel A, bottom panels) where membrane curvature occurred within the detecting kernel number 2. The membrane surface area was measured as a curvature length multiplied by the thickness of the confocal optical section (2 μm). The increase in local membrane area accompanied the increase in focal fluorescence intensity until 130 s beyond which it saturated, similar to the change in fluorescence intensity (middle trace in panel B). That the increase in membrane area was not due to phototoxic damage was suggested by the observation that the formation of membrane blebs, seen after long periods of laser scanning were not associated with local increase in fluorescence intensity.

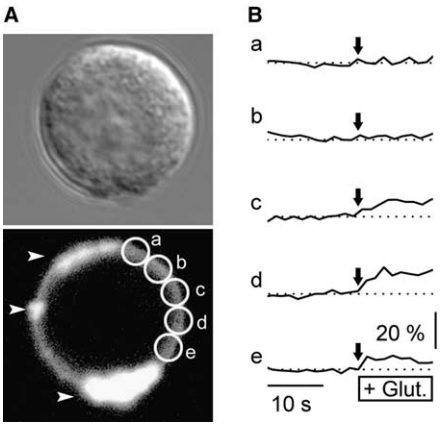

Fig. 2. Mapping the perimeter of a melanotroph membrane for increase in fluorescence intensity. (A) Differential interference contrast image of the melanotroph (top) and the corresponding confocal detection of FM1–43 fluorescence (bottom). The panel shows the positions of the different detection kernels consisting of circular image fields of 2 μm diameter. Arrowheads mark the bright spots on the membrane surface, representing hormone deposition on the cell surface, which were discarded from the analysis. Panel B shows the time course of the fluorescence intensity in the marked areas (panel A), following addition of glutamate (arrow) to the recording chamber (400 μM). The centre of the circular image field was positioned at the outer edge of the rim of the cell, and bright fluorescent regions with hormone adherent to the cell surface were excluded from the analysis. Images were analysed after 30 s of commencing fast *xy* scan, during which the decrease in fluorescence due to photobleaching was found to reach a steady state exponentially (time-constant of 8.3 s) in control experiments ($N = 12$, not shown). Note that constant fluorescence intensity levels in traces c, d, and e increased after stimulation with glutamate (arrows) by approximately 15% of the basal intensity level, which indicates stimulation of exocytosis in corresponding, previously silent, areas. The horizontal scale bar represents time of 10 s and the vertical scale bar represents the 20% change of fluorescence relative to the basal fluorescence of the region of interest.

3. Results

3.1. Spontaneous time-dependent changes in FM1–43 fluorescence intensity reveal distinct exocytotic membrane domains

Time-dependent fluorescence intensity changes were mapped by using a detection kernel of fixed dimension (see Fig. 1A). These measurements revealed highly localized, spontaneous time-dependent FM1–43 fluorescence changes (Fig. 1B). In some experiments relatively intense localized fluorescent changes were recorded accompanied by a local increase in the membrane curvature (Fig. 1A and C). This appears to be an outcome of massive local exocytosis, since the increase in membrane surface area (Fig. 1C) appears to be correlated with the increase in fluorescence intensity (Fig. 1B, middle trace). In addition, the time-dependent increase in FM1–43 fluorescence intensity may be contributed by the deposition of the vesicle cargo on the cell surface. On the site 3 (Fig. 1A and B, bottom trace), there was no significant change in fluorescence intensity. The local regions showing spontaneous time-dependent change in FM1–43 fluorescence intensity represent sites of preferential fusion of vesicles with the plasma membrane that leads to the secretion of vesicle cargo. These specialized areas are termed exocytotic domains.

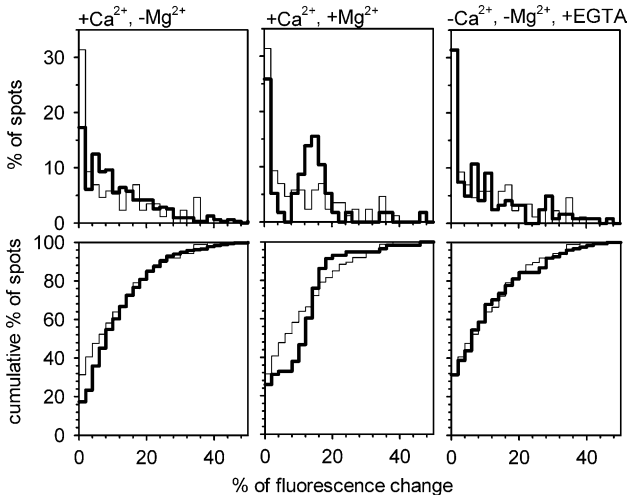

Fig. 3. Cell stimulation by glutamate recruits new exocytotic domains and enhances the activity of the spontaneously active exocytotic domains. Comparison of local FM1–43 fluorescence intensity increase by glutamate. Top row: Histogram distribution of localized fluorescence intensity increase after glutamate application (thick line) in different ionic conditions and in control (thin line). The histogram plots are combined distributions from multiple independent experiments (for number of cells (N) and spots (n) analysed, see below) of the kind shown in Fig. 2. The data are expressed as percentage increase in fluorescence as follows: relative changes in exocytosis were estimated as percentage change in fluorescence intensity estimated at five time points immediately before addition of glutamate and the peak intensity between 10 and 60 s after addition of glutamate. The control distribution was obtained from no stimulus runs, and applications of equal volumes of external bath solution used for glutamate stimulation, containing Mg^{2+}-free solution with Ca^{2+} and dopamine (200 nM). The other three distributions relate to glutamate stimulation in the presence of Ca^{2+} and absence of Mg^{2+} in the bath ($+Ca^{2+}$, $-Mg^{2+}$), in the presence of both Ca^{2+} and Mg^{2+} ($+Ca^{2+}$, $+Mg^{2+}$), and in the absence of both Ca^{2+} and Mg^{2+} with added presence of EGTA ($-Ca^{2+}$, $-Mg^{2+}$, +EGTA). In control, $N = 15$, $n = 93$; glutamate in bath solution with $+Ca^{2+}$, $-Mg^{+2}$, $N = 39$, $n = 313$; $+Ca^{2+}$, $+Mg^{2+}$, $N = 6$, $n = 58$ and in $-Ca^{2+}$, $-Mg^{2+}$, + EGTA, $N = 19$, $n = 130$. Descriptive analysis of the frequency histograms did not show normal distribution of frequency of observations over percentage increase in fluorescence, for the four different data sets, viz. control (Mean = 9.41, S.D. = 10.27, kurtosis = 0.06, skewness = 0.99), and following application of glutamate in the presence (Mean = 10.72, S.D. = 9.33, kurtosis = 2.64, skewness = 1.15) or absence of Mg^{2+} (Mean = 11.17, S.D. = 10.12, kurtosis = 1.46, skewness = 1.25) in Ca^{2+} containing solution, and in Ca^{2+}- and Mg^{2+}-free external soln. (Mean = 9.98, S.D. = 9.02, kurtosis = 0.63, skewness = 1.21). To further confirm that the four different data sets were indeed not drawn from a normal distribution, the Shapiro–Wilk test was done for normality, and the test confirmed significant departures from a normal distribution. Bottom row: Cumulative frequency plot of percentage fluorescence change in control and following glutamate application under different ionic conditions. The cumulative frequency plot was constructed from the histogram data shown in the top row. A Kolmogrov–Smirnov test was performed on the cumulative distributions to understand whether the responses to glutamate are sensitive to Mg^{2+} and require the presence of Ca^{2+} in the extracellular solution. For each of these tests, the results were compared to the control data set in the absence of glutamate. The parameter D (standing for difference) in the Kolmogrov–Smirnov test, gives the difference between the cumulative distributions of the data points, and p is the level of significance. For the glutamate induced response in the presence and absence of Mg^{2+} in the external medium containing Ca^{2+}, $D = 0.242$, $p = 0.028$ and $D = 0.224$, $p = 0.002$; respectively; while in the absence of Mg^{2+} in a Ca^{2+}-free solution, $D = 0.09$ and $p = 0.83$.

3.2. Frequency distributions of local time-dependent changes in fluorescence intensity and distinct fusion-competent sites in the plasma membrane

We mapped the membrane along the cell perimeter using a detection kernel of fixed dimension (see Fig. 1A). Bright spots on the membrane surface, representing hormone deposition on the cell surface, did not show time-dependent changes in the fluorescence intensity, and were not included in the analysis (Figs. 1A and 2A, arrowheads). Firstly, the time-dependent change in fluorescence intensity was evaluated for a large number of such sites in different cells under basal conditions. The distribution of spontaneous fluorescence intensity increases of localized membrane domains revealed significant heterogeneity with an average amplitude of around 15% (Fig. 3, thin lines), reflecting important local variations in the state of secretory activity and/or structural components associated with vesicle fusion. Secondly, to test whether discrete regions in the cell perimeter can respond to a physiological stimulus by a change in FM1–43 fluorescence, we stimulated the cells with glutamate, which causes elevation of intracellular [Ca^{2+}] [3]. The fluorescence intensity following glutamate application increased to a new steady state (Fig. 2). In all experiments irrespective of the age of the cells in culture, and conditions used for stimulation, an increase in FM1–43 fluorescence intensity could be elicited only from a subset of distinct membrane areas. Histograms of the local responses from a large number of membrane regions, i.e., putative exocytotic domains, are shown in Fig. 3. Note that all the frequency histograms cannot be described by a normal distribution. A normal distribution would indicate that the activity of exocytotic domains is homogeneously distributed on the plasma membrane. Further, in a substantial number of membrane areas encircled by detecting kernels, no change in fluorescence was detected, which indicates inactive regions in the membrane, sites devoid of hormone release. A pertinent argument against this observation could be that the responses have been picked from cells which show different levels of basal exocytotic activity, i.e., cells showing low basal activity would have a higher number of inactive membrane sites studied by the detection kernels. However, analysis of percentage fluorescence change per cell by pooling the fluorescence change in all detection kernels per cell, showed that the detection kernels did not show a fluorescence change in less than 3% of cells. Moreover, the modal value of fluorescence intensity change was 8%. This suggests that there are distinct fusion-competent sites in the plasma membrane of rat neuroendocrine melanotrophs.

3.3. Recruitment and activation of putative exocytotic membrane domains by glutamate stimulation

The stimulation of cells by glutamate significantly altered the shape of the distribution of localized membrane fluorescence intensity increases (Fig. 3). The analysis of cumulative distributions suggests that glutamate stimulation of exocytotic domains is sensitive to Mg^{2+} and requires the presence of Ca^{2+} in the external medium (compare distributions in Fig. 3, lower panels), which suggests the involvement of ionotropic glutamate receptor [3]. The middle distribution histogram (Fig. 3, upper middle; $+Ca^{2+}$, $+Mg^{2+}$) shows an increase in the mid-range of the histogram, in glutamate stimulated cells (thick line) compared to control experiments (thin line). This mid-range of the histogram corresponds to the membrane domains with about 15% increase in the fluorescence intensity. On the other hand, this histogram also shows a reduction in the region at about 7% increase in the fluorescence intensity. We suggest that glutamate elevates secretory activity from spontaneously active exocytotic domains. These conditions with the Mg^{2+} present would activate the ionotropic non-NMDA receptors. It is important to note that substantial number of sites was observed where fusion did not occur. This is represented as the peak at the farthest left in all upper histograms. There was however a decrease in the number of sites showing failures, in the presence of glutamate and Ca^{2+} and the absence of Mg^{2+} (Fig. 3, thick line, upper left panel). These conditions would also activate the ionotropic NMDA glutamate receptors.

In order to understand whether the stimulation of exocytotic domains is dependent on the initial level of exocytotic activity, the relative starting fluorescence for kernels showing a 5–50% increase in fluorescence intensity was normalized with the averaged initial fluorescence intensity of all cells. The relative starting fluorescence intensity was significantly higher in cases of putative exocytotic domains where the glutamate response was present (Fig. 4A), which indicates that glutamate stimulates previously spontaneously active exocytotic domains as depicted in the model (Fig. 4B). The model in addition shows that glutamate may also recruit inactive exocytotic domains, as suggested by the data presented in Fig. 3.

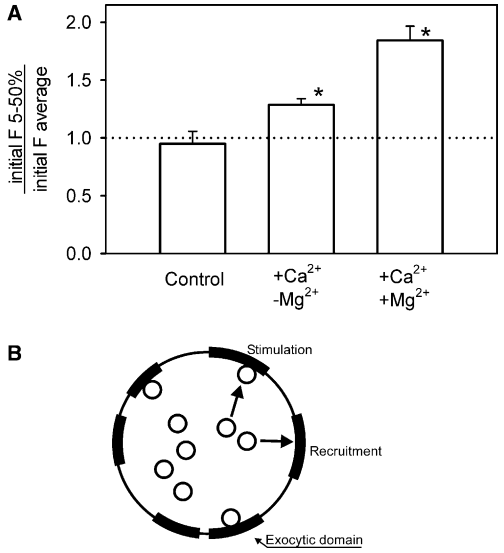

Fig. 4. (A) Relative localized starting fluorescence intensity in detection kernels showing secretory activity. Histogram showing the initial fluorescence intensity (initial F) in the kernels showing a 5–50% increase in fluorescence normalized with the average of initial fluorescence intensity (initial F average) in all the kernels. Measurements of changes in fluorescence intensity in kernels in cells under basal conditions (Control) are compared with cells stimulated by the glutamate in the absence of Mg^{2+} ($+Ca^{2+}$, $-Mg^{2+}$) or in the presence of Mg^{2+} ($+Ca^{2+}$, $+Mg^{2+}$). Asterisk, $P < 0.01$, Student's t test. The histogram is obtained from the analysis of the data shown in Fig. 3. (B) Model summarizing the effect of stimulation on the activity of exocytotic membrane domains (thick line) of endocrine cell. Stimulation depicts the activation of the already spontaneously active exocytotic domain. Recruitment depicts the recruitment of an inactive exocytotic domain.

4. Discussion

The styryl dye FM1–43 was used to stain membranes of rat pituitary melanotrophs to monitor exocytosis. The very bright FM1–43 stained patches in the cell perimeter appeared to be qualitatively different from the fluorescence observed in the plasma membrane, typically with fluorescence intensities several fold higher than the rest of the membrane. These membrane areas were devoid of time-dependent changes in FM1–43 fluorescence and represent staining of vesicle content (not shown), as observed in pituitary lactotrophs [23].

The frequency histograms in Fig. 3 do not show a normal distribution, and suggests that stimulation of melanotrophs with glutamate does not induce uniform fusion of vesicles along the cell perimeter. A patchy distribution of α-MSH antibody around the cell perimeter was observed (data not shown) that may be due to a patchy distribution of glutamate- and KCl-stimulated calcium sources in the plasma membrane [24] that trigger the release of uniformly distributed secretory machinery in the plasma membrane. However, this is unlikely, since the application of glutamate and KCl did not result in distinct "hot-spots" of local increases in $[Ca^{2+}]_i$ using fura-2 imaging of melanotrophs (not shown), consistent with previous reports [25]. Moreover, dialysis of different calcium buffers into melanotrophs revealed a relatively large distance between calcium sources and calcium receptors of the secretory apparatus [26,27].

Heterogeneity in the response amplitudes was observed without stimulation (basal secretion) and following stimulation with glutamate in FM1–43 stained plasma membrane. A substantial number of sites were observed where fusion did not occur. The fraction of sites showing failures decreased upon activation of glutamate receptors (Fig. 3). Sites can show failures if the recycled vesicles mix with the total vesicle pool without maintaining a hierarchy of releasibility [28]. Stimulation with glutamate increased the number of active exocytotic sites by the recruitment of inactive sites and increased activity of exocytotic domains that are already present at basal conditions (Figs. 3 and 4B). The distribution histogram in Fig. 3 where cells were stimulated with glutamate in the presence of $+Ca^{2+}$ and $+Mg^{2+}$ shows an increase in the midrange of the histogram, which corresponds to the membrane domains with about 15% increase in the fluorescence intensity. These conditions with the Mg^{2+} present would activate the ionotropic non-NMDA receptors. On the other hand, the peak at the farthest left in the presence of glutamate and Ca^{2+} and the absence of Mg^{2+} is decreased, which shows that new fusion sites are recruited due to the activation of the ionotropic NMDA glutamate receptors.

Previous work has shown that stimulation of the ionotropic glutamate receptors by both AMPA and NMDA increased intracellular calcium, compared to the activation of metabotropic glutamate channels [3]. In the melanotrophs, glutamate application in the absence of external calcium, failed to elicit responses significantly different from the control (Fig. 3), which suggests the critical role of calcium in biasing a cell towards stimulus-dependent secretion, despite having robust cellular machinery for basal secretion.

Studies on the dynamics of vesicle fusion with the plasma membrane using total internal reflection fluorescence microscopy have suggested the existence of 'active zones' for secretion, where a high percentage of vesicle fusion occurs spatially close to another fusion [12]. Our experimental results suggest that several such preferred sites exist spatially closer to each other in the melanotrophs, to form exocytotic domains, whose activity results in the export and deposit of the vesicle content on the surface of the plasma membrane.

The molecular nature of FM1–43 stained exocytotic domains observed in our experiments is not clear, but may constitute of among other candidates the SNARE molecules [29]. For fusion to take place vesicle and plasma membrane should be close enough for v- and t-SNARES to touch and initiate formation of the coiled complex. Small patches of SNAREs in the plasma membrane lawns of PC12 cells separated by distances greater than 2 μm have been reported by Lang et al. [30]. Although a clear correspondence between this observation and the exocytotic domains cannot be drawn, the patchy distribution of SNAREs can nevertheless contribute to the activity of the exocytotic domains. The role of the SNARE complex in regulated exocytosis in melanotrophs was shown previously [31], although the subcellular distribution of t-SNARE (Syntaxin I) in rat melanotrophs is rather uniform [32]. A subset of dense core vesicles in melanotrophs specifically stains for CAPS (Ca-dependent activator protein for secretion) that mediate the high Ca^{2+}-sensitivity exocytosis in melanotrophs [31]. A similar role was found for synaptotagmin I [33]. Immunostaining for CAPS suggests a non-uniform distribution of CAPS stained vesicles in the subplasmalemmal membrane, appearing as punctate stains. This property may contribute to the establishment of functional exocytotic domains.

In summary, the optical approach to monitor the secretory activity of a single peptide secreting neuroendocrine cell revealed that basal and stimulated hormone secretion takes place at distinct membrane domains. These specialized membrane locales, reminiscent of active zones in nerve terminals, maybe involved in limiting the secretory capacity of neuroendocrine cells.

Acknowledgement: This work was supported by the Grant #P3 310 0381 of The Ministry of Education, Sciences and Sports of The Republic of Slovenia, the #Z3-3510-1683 Grant, and the R01 NS36665-05 Grant. S.K.S. was supported by a grant from The Ministry of Education, Sciences and Sports of The Republic of Slovenia.

References

[1] Douglas, W.W. and Taraskevich, P.S. (1985) The electrophysiology of adenohypophyseal cells in: The Electrophysiology of the Secretory Cell (Poisner, A.M. and Trifaro, J.M., Eds.), pp. 63–92, Elsevier, Amsterdam.
[2] Taraskevich, P.S. and Douglas, W.W. (1990) Dopamine (D2) or γ-aminobutyric acid (GABAB) receptor activation hyperpolarizes rat melanotrophs and pertussis toxin blocks these responses and the accompanying fall in Ca^{2+}. Neurosci. Lett. 112, 205–209.
[3] Giovannucci, D.R. and Stuenkel, E.R. (1995) Glutamate receptor agonists modulate $[Ca^{2+}]_i$ in isolated rat melanotropes. Neuroendocrinology 62, 111–122.
[4] Zupančič, G., Kocmur, L., Veranič, P., Grilc, S., Kordaš, M. and Zorec, R. (1994) The separation of exocytosis from endocytosis in rat melanotroph membrane capacitance records. J. Physiol. 480, 539–552.
[5] Kreft, M. and Zorec, R. (1997) Cell-attached measurements of attofarad capacitance steps in rat melanotrophs. Pflugers Arch. 434, 212–2144.

[6] Paras, C.D. and Kennedy, R.T. (1995) Electrochemical detection of exocytosis at single rat melanotrophs. Anal. Chem. 67, 3633–3637.
[7] Zhang, X., Ogorevc, B., Rupnik, M., Kreft, M. and Zorec, R. (1999) Cathophoresis paint insulated carbon fibre microdisk electrode and its application to in vivo amperometric monitoring of quantal secretion from single rat melanotrophs. Anal. Chem. Acta 378, 135–143.
[8] Thomas, P., Surprenant, A. and Almers, W. (1990) Cytosolic Ca^{2+}, exocytosis, and endocytosis in single melanotrophs of the rat pituitary. Neuron 5, 723–733.
[9] Thomas, P., Wong, J.G. and Almers, W. (1993) Millisecond studies of secretion in single rat pituitary cells stimulated by flash photolysis of caged Ca^{2+}. EMBO J. 12, 303–306.
[10] Parsons, T.D., Coorssen, J.R., Horstmann, H. and Almers, W. (1995) Docked granules, the exocytic burst, and the need for ATP hydrolysis in endocrine cells. Neuron 15, 1085–1096.
[11] Plattner, H., Artalejo, A.R. and Neher, E. (1997) Ultrastructural organization of bovine chromaffin cell cortex-analysis by cryofixation and morphometry of aspects pertinent to exocytosis. J. Cell Biol. 139, 1709–1717.
[12] Zenisek, D., Steyer, J.A. and Almers, W. (2000) Transport, capture and exocytosis of single synaptic vesicles at active zones. Nature 406, 849–854.
[13] Cuchillo-Ibanez, I., Michelena, P., Albillos, A. and Garcia, A.G. (1999) A preferential pole for exocytosis in cultured chromaffin cells revealed by confocal microscopy. FEBS Lett. 459, 22–26.
[14] Wick, P.F., Trenkle, J.M. and Holz, R.W. (1997) Punctate appearance of dopamine-beta-hydroxylase on the chromaffin cell surface reflects the fusion of individual chromaffin granules upon exocytosis. Neuroscience 80, 847–860.
[15] Gil, A.G., Viniegra, S., Neco, P. and Gutierrez, L.M. (2001) Co-localisation of vesicles and P/Q Ca^{2+}-channels explains the preferential distribution of exocytotic active zones in neurites emitted by bovine chomaffin cells. Eur. J. Cell Biol. 80, 358–365.
[16] Schroeder, T.J., Jankowski, J.A., Senyshyn, J., Holz, R.W. and Wightman, R.M. (1994) Zones of exocytotic release on bovine adrenal medullary cells in culture. J. Biol. Chem. 269, 17215–17220.
[17] Robinson, I.M., Finnegan, J.M., Monck, J.R., Wightman, R.M. and Fernandez, J.M. (1995) Colocalisation of calcium entry and exocytotic release sites in adrenal chromaffin cells. Proc. Natl. Acad. Sci. USA 92, 2474–2478.
[18] Robinson, I.M., Yamada, M., Carrion-Vazquez, M., Lennon, V.A. and Fernandez, J.M. (1996) Specialized release zones in chromaffin cells examined with pulsed laser imaging. Cell Calcium 20, 181–201.
[19] Betz, W.J., Mao, F. and Smith, C.B. (1992) Activity-dependent fluorescent staining and destaining of living vertebrate motor nerve terminals. J. Neurosci. 12, 363–375.
[20] Smith, C.B. and Betz, W.J. (1996) Simultaneous independent measurement of endocytosis and exocytosis. Nature 380, 531–534.
[21] Mains, R.E. and Eipper, B.A. (1979) Synthesis and secretion of corticotropins, melanotropins and endorphins by rat intermediate pituitary cells. J. Biol. Chem. 254, 7885–7894.
[22] Rupnik, M. and Zorec, R. (1992) Cytosolic chloride ions stimulate Ca(2+)-induced exocytosis in melanotrophs. FEBS Lett. 303, 221–223.
[23] Angleson, J.K., Cochilla, A.J., Kilic, G., Nussinovitch, I. and Betz, W.J. (1999) Regulation of dense core release from neuroendocrine cells revealed by imaging single exocytic events. Nat. Neurosci. 2, 2440–2446.
[24] Monck, J.R., Robinson, I.M., Escobar, A.L., Vergara, J.L. and Fernandez, J.M. (1994) Pulsed laser imaging of rapid Ca^{2+} gradients in excitable cells. Biophys. J. 67, 505–514.
[25] Fisher, T.E. and Fernandez, J.M. (1999) Pulsed laser imaging of Ca^{2+} influx in a neuroendocrine terminal. J. Neurosci. 19, 7450–7457.
[26] Neher, E. (1998) Vesicle pools and Ca^{2+} microdomains: new tools for understanding their roles in neurotransmitter release. Neuron 20, 389–399.
[27] Mansvelder, H.D. and Kits, K.S. (2000) Calcium channels and the release of large dense core vesicles from neuroendocrine cells: spatial organization and functional coupling. Progr. Neurobiol. 62, 427–441.
[28] Ryan, T.A. and Smith, S.J. (1995) Vesicle pool mobilization during action potential firing at hippocampal synapses. Neuron 14, 988–989.
[29] Jahn, R. and Grubmuller, H. (2002) Membrane fusion. Curr. Opin. Cell Biol. 14, 488–495.
[30] Lang, T., Margittai, M., Holzler, H. and Jahn, R. (2002) SNAREs in native plasma membranes are active and readily form core complexes with endogenous and exogenous SNAREs. J. Cell Biol. 158, 751–760.
[31] Rupnik, M., Kreft, M., Sikdar, S.K., Grilc, S., Romih, R., Zupancic, G., Martin, T.F. and Zorec, R. (2000) Rapid regulated dense-core vesicle exocytosis requires the CAPS protein. Proc. Natl. Acad. Sci. USA 97, 5627–5632.
[32] Kreft, M., Gasman, S., Chasserot-Golaz, S., Kuster, V., Rupnik, M., Sikdar, S.K., Bader, M.-F. and Zorec, R. (1999) The heterotrimeric Gi3 protein acts in slow but not in fast exocytosis of rat melanotrophs. J. Cell. Sci. 112, 4143–4150.
[33] Kreft, M., Kuster, V., Grilc, S., Rupnik, M., Milisav, I. and Zorec, R. (2003) Synaptotagmin I increase the probability of vesicle fusion at low (Ca^{2+}) in pituitary cells. Am. J. Physiol. Cell Physiol. 284, C547–C554.